ISSN 0021-3640, JETP Letters. ©The Authors(s), 2024. This article is an open access publication.

Frequency Conversion of Femtosecond Ti:sapphire Laser Pulse to the Long-wave Mid-IR Range with $BaGa_2GeSe_6$ Crystal

I. O. Kinyaevskiy[1)], *A. V. Koribut, Ya. V. Grudtsyn, M. V. Ionin*

P. N. Lebedev Physical Institute of the Russian Academy of Sciences, 119991 Moscow, Russia

Submitted 4 April 2024
Resubmitted 4 April 2024
Accepted 13 April 2024

Generation of ultrashort mid-IR pulses spanning from 8.5 to 10.5 μm with high energy (up to 4.5 μJ) was experimentally demonstrated through difference frequency generation in $BaGa_2GeSe_6$ crystal pumped by 100-fs 0.95-μm Ti:sapphire laser pulses. Optical damage threshold and two-photon absorption coefficient were determined for this pump pulses. Frequency conversion efficiency reached 0.24 % at 1.85 mJ pump pulse energy and was decreased at higher one. Estimations indicate that application of 15 mm in diameter wide-aperture $BaGa_2GeSe_6$ sample will allow one to increase pump pulse energy up to $\sim$10 mJ, and to increase the mid-IR pulse energy up to 24 μJ at the same efficiency.

DOI: 10.1134/S0021364024600988

The development of femtosecond long-wave mid-infrared (mid-IR) (6–12 μm) laser sources is of great interest for many applications in fundamental and applied fields such as particle acceleration [1], attosecond pulse generation [2], remote gas analysis [3], crystals modification [4], inactivation of pathogenic bacteria [5] and others. One of the main techniques to produce the mid-IR femtosecond laser pulse is spectrum conversion of reliable short-wave lasers in nonlinear crystals via difference-frequency generation (DFG) or optical parametric oscillation (OPO) [6–11]. Mostly such systems are based on a laser with a high pulse repetition rate that provided relatively-high average power of radiation at low peak power/energy of the pulses [7–9]. Therefore, the energy of the femtosecond mid-IR pulses in this case is low, about at pJ [9] or nJ [7] level. Our research is focused on the development of a femtosecond long-wave mid-IR laser system with pulse energy at μJ-level whose peak power will exceed the critical power of self-focusing for mid-IR materials (tens of MW). Thus, we selected a femtosecond Ti:sapphire laser as a future front-end laser because of its well-developed technology, which allows one to produce 10 PW laser pulses [12].

As a nonlinear crystal we selected the promising recently developed $BaGa_2GeSe_6$ (BGGSe) crystal [13, 14] due to its appropriate transmittance, high nonlinearity, favorable dispersion and high optical damage threshold. Detailed characterization of linear and nonlinear optical properties for the BGGSe crystal can be found in [13, 14]. Recently, this material was successfully used for frequency conversion of femtosecond [9] and nanosecond [10] near-IR laser pulses to the mid-IR range, as well as for frequency conversion of microsecond CO laser [11]. Our BGGSe crystal sample of $7 \times 7 \times 0.6$ mm size was grown at the High Technologies Laboratory of the Kuban State University by D. V. Badikov and V. V. Badikov. It was cut at $\theta = 29°$, $\varphi = 42.7°$ for type-I frequency mixing (see Fig. 1). For comparison, we also considered the traditional $AgGaS_2$ (AGS) crystal as a reference material. The AGS sample of $7 \times 8 \times 2$ mm size, that was grown at the Institute of Geology and Mineralogy, SB RAS, was cut at $\theta = 43°$, $\varphi = 0°$ (for the type-II phase-matching, see Fig. 1). It should be noted that BGGSe and AGS have similar bandgap: 2.38 eV [13] and 2.62 eV [15], respectively.

The calculated phase-matching angles for DFG of Ti:sapphire laser pulse ($\lambda = 0.95\,\mu$m) and near-IR supercontinuum ($\lambda = 1.0{-}1.2\,\mu$m) are presented in Fig. 1a: type-I ($o - e \to e$) phase-matching for BGGSe and type-II ($e - o \to e$) phase-matching for AGS. The phase-matching angle calculation is a "standard" procedure that can be found, for example, in handbook [15]. Dispersion equations of BGGSe and AGS crystals were taken from [14] and [15], respectively. In addition, the square of effective nonlinearity depending on azimuthal angle φ was calculated and presented in Fig. 1b. For BGGSe, effective nonlinearity was calculated as $d_{\text{eff}} = (d_{11} \sin 3\varphi + d_{22} \cos 3\varphi) \cos^2 \theta$, where $d_{11} = 23.6$ pm/V, $d_{22} = -18.5$ pm/V [14]. For AGS, it was calculated as $d_{\text{eff}} = d_{36} \sin 2\theta \cos 2\varphi$, where $d_{36} = 12.5$ pm/V [15]. Figure 1 shows that the BGGSe cut angle corresponds to DFG wavelength of 10 μm, the

[1)]e-mail: kinyaevskiyio@lebedev.ru

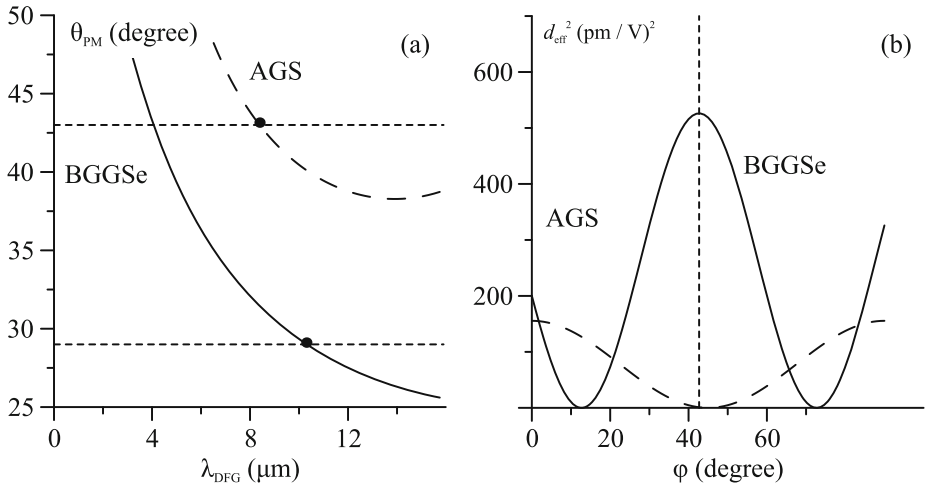

Fig. 1. Calculated phase-matching angles for DFG (a) and the square of effective nonlinearity (b) in BGGSe (solid line) and AGS (dashed line) crystals

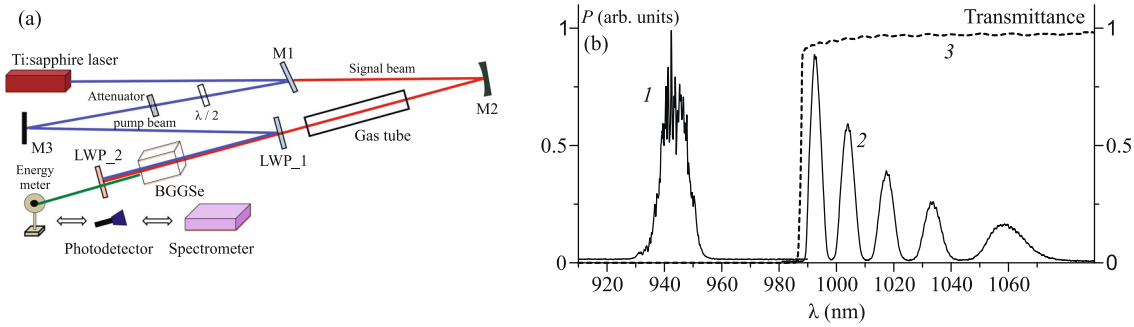

Fig. 2. (Color online) (a) – Optical scheme of the experiment, see text for details. (b) – Spectra of pump (1) and signal (2) pulses, and transmittance of LWP_1 filter (3)

AGS cut angle corresponds to DFG wavelength of 8 μm. The angle φ is optimized for both crystals. The square of effective nonlinearity for BGGSe is 3.4 times higher than that for AGS, and the BGGSe should be 3.4 times more efficient, respectively.

The optical scheme of our experiment is presented in Fig. 2a. We used the Ti:sapphire laser "START-480M" (Avesta Project Ltd., Russia) with pulse energy up to 10 mJ, central wavelength $\lambda \approx 0.95\,\mu$m, spectral width at FWHM ~ 12 nm, pulse duration of 100 fs, pulse repetition rate – 10 Hz. The laser beam was split into two arms by partly-transmitting mirror (M1) – reflecting one with high pulse energy ($E \approx 9.3$ mJ) as a pump beam, and transmitting one with lower energy ($E \approx 0.7$ mJ) as a signal beam.

The pump pulse energy was controlled by a variable diffraction attenuator. Its polarization was tuned by 90° with a half-wave plate because it had to be ordinary wave in the BGGSe (when AGS crystal was used, the signal beam polarization was tuned). The signal beam was focused by spherical mirror (M2, the focal length of 2 m) into a gas tube of 1.46 m length filled by CO_2 at 3 atm gas pressure where the laser pulse was broadened due to self-phase modulation under filamentation. Then, the pump and signal pulses were combined together. The time correlation of the pump and signal pulses was controlled by the pump pulse arm length through the adjustment of mirror M3 position.

The spatial alignment was implemented by longwave pass filter LP02-980RU-25 (Semrock, USA), LWP_1 in Fig. 2a. The filter had reflectance $> 99.9\,\%$ for the pump pulse and transmittance $> 95\,\%$ for the signal pulse. The pump and signal pulse spectrum after the filter are presented in Fig. 2b as well as the filter transmittance. After the filter, the signal pulse energy was 0.15 mJ, the pump pulse energy could be up to ~ 9 mJ.

The combined laser pulse was sent into a nonlinear crystal (BGGSe or AGS) without any focusing. The beam diameter of pump and signal pulses at the crystal were 4.1 mm and 4.5 mm at $1/e^2$ level, respectively.

The mid-IR pulse generated in a nonlinear crystal was separated from the near-IR radiation by longwave pass filter (# 5 from a set of filters of IR spectrometer IKS-31, LOMO, Russia), LWP_2 in Fig. 2a. The filter had transmittance 50 % for wavelengths of 5–14 μm and absolutely suppressed near-IR radiation. The mid-IR radiation was detected with photodetector PEM-L-3 (VIGO systems, Poland), spectra were measured by a home-made spectrometer based on a diffraction grating with 75 groves/mm equipped with photodetector PEM-L-3, average DFG pulse energy was measured with Ophir-3A power meter.

First, the optimal crystals orientation was found. The dependence of the DFG pulse power/energy on the angle of incidence (α) on the BGGSe crystal is presented in Fig. 3. This angle was recalculated into the angle

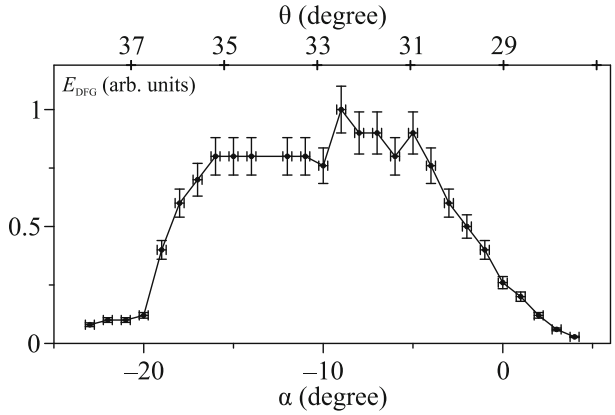

Fig. 3. Dependence of the DFG pulse energy on the angle of incidence on the BGGSe crystal (θ), upper X-axis is phase-matching angle θ

θ between the pump wavevector and the crystal optical axis, upper X-axis in Fig. 3. The dependence has a plateau at $\theta = 30° - 36°$ which, according to Fig. 1a, corresponds to DFG wavelength tuning from 7.5 μm to 10.5 μm, lower θ corresponds to a longer wavelength. A drop of the detected DFG energy at $\theta \leq 29°$ could be related with Manley–Rowe relation decrease at DFG spectrum shift to longer wavelengths. A drop of DFG energy at $\theta \geq 36°$ was related with DFG spectrum shift to shorter wavelengths which required longer wavelengths in the signal pulse spectrum. However, the signal pulse power had a notable decrease at $\lambda > 1070$ nm (see Fig. 2b).

Next, the relative DFG pulse energy (the signal magnitude at the photodetector) was measured as a function of the pump pulse energy at the optimal angle of the crystal samples ($\alpha = -10°$ for BGGSe, and $\alpha = -14°$ for AGS), see Fig. 4. With an increase in energy up to a certain value, this dependence had a linear trend

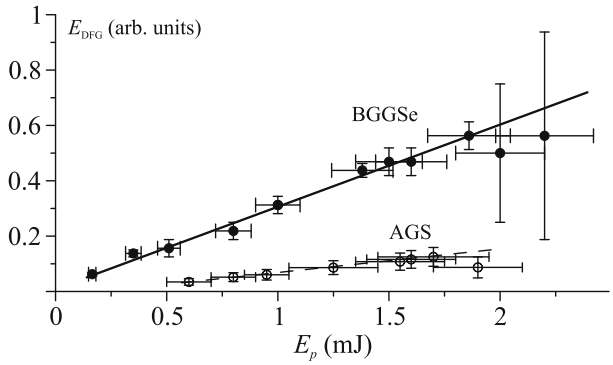

Fig. 4. Relative DFG pulse energy vs pump pulse energy at the optimal position of the BGGSe and AGS crystal

for both crystals which is in accordance with theory of parametric frequency conversion (see, for example, [15]). However, the BGGSe crystal appeared to be about 5 times more efficient than AGS. In BGGSe, at high pump pulse energy $E_p \geq 2$ mJ the magnitude of the strongest DFG pulses was increased, however, pulse-by-pulse stability became low, which resulted in decreased average DFG pulse energy. The evident optical damage of BGGSe sample surface was observed at $E_p \approx 2.5$ mJ that coresponds to fluence of 0.04 J/cm^2 and intensity of 0.4 TW/cm^2. It should be noted that the decrease of the average DFG pulse energy was also observed in AGS crystal at $E_p \approx 1.8$ mJ.

The nature of this instability and DFG energy decrease is not clear for us. One of the reasons can be related with a nonlinear absorption and plasma formation, respectively, that causes reflection/scattering/absorption of the longwave mid-IR pulse. The dependence of BGGSe transmittance on pump pulse energy is presented in Fig. 5. Even at

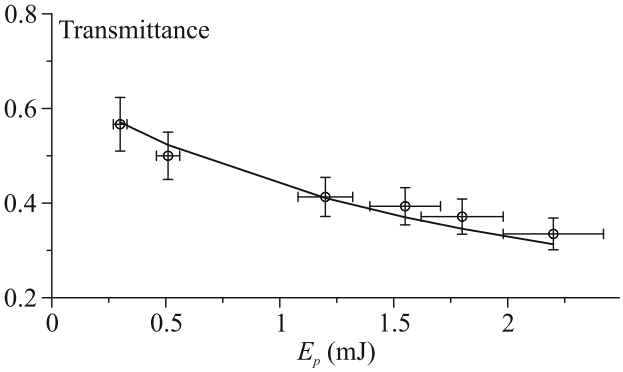

Fig. 5. Transmittance of BGGSe crystal vs pump pulse energy

$E_p = 0.25$ mJ the transmittance is notably lower than one determined just by Fresnel reflection (70 %). At $E_p = 2$ mJ the transmittance was decreased down to $\sim$35 %. The line in Fig. 5 is the calculated trans-

mittance of the sample at two-photon coefficient $\beta = 0.25\,\mathrm{cm/GW}$ which provided the best agreement with the experiment. This value is 5–10 times less than that presented in [14].

To measure an absolute value of DFG pulse energy, Ophir-3A power meter was used. The average DFG pulse energy was determined as average DFG power divided by pulse repetition rate (10 Hz) taking into account the transmittance of LWP_2 filter. Average DFG pulse energy obtained with BGGSe at $E_p = 1.85\,\mathrm{mJ}$ was $4.5 \pm 0.5\,\mu\mathrm{J}$. This energy corresponds to DFG efficiency of 0.24 % which is comparable with one obtained with high repetition rate low-energy laser systems like in [9]. Taking into account a possibility to increase pump pulse energy of our setup up to $\sim 10\,\mathrm{mJ}$, the DFG pulse energy can be increased up to $\sim 24\,\mu\mathrm{J}$ at the same efficiency, however, it required a wide-aperture, $\sim 15\,\mathrm{mm}$ in diameter BGGSe sample. Average DFG pulse energy in AGS was not confidently measured with Ophir-3A power meter due to its low signal.

The spectrum of DFG pulse obtained in BGGSe under optimal conditions ($\alpha = -10°$, at $E_p = 1.85\,\mathrm{mJ}$) is presented in Fig. 6. It was measured pulse-by-pulse

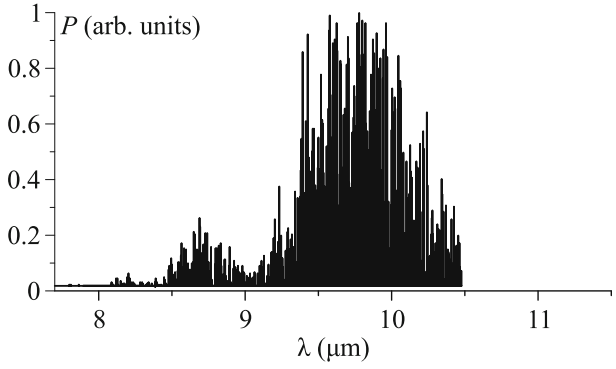

Fig. 6. Spectrum of DFG pulse obtained in BGGSe crystal at $\alpha = -10°$

by a slow diffraction grating rotation of the home-made mid-IR spectrometer. The DFG spectrum spanned from $8.5\,\mu\mathrm{m}$ to $10.5\,\mu\mathrm{m}$ at the level of 0.1 of the power maximum, which was in accordance with results of [9] and confirmed BGGSe applicability of producing few-cycle mid-IR pulses. However, DFG spectrum had a minor hump at $8.7\,\mu\mathrm{m}$ wavelength which took origin from a hump structure in the signal pulse spectrum (see Fig. 2b). Therefore, to optimize the DFG spectrum shape, the spectrum of the signal pulse should be more uniform.

Thus, DFG of 100-fs 0.95-μm laser pulses with energy over 1 mJ was studied in BGGSe crystal. The optical damage of BGGSe was observed at $0.04\,\mathrm{J/cm^2}$ pump pulse fluence. The measured two-photon coefficient was $0.25 \pm 0.05\,\mathrm{cm/GW}$. The ultrashort mid-IR pulse spanning from 8.5 to $10.5\,\mu\mathrm{m}$ with energy up to $4.5\,\mu\mathrm{J}$ was obtained. Taking into account pump pulse duration of 100 fs, this energy corresponds to peak power of 45 MW which exceeds self-focusing critical power in solids, e.g. in ZnSe [16], and such pulses can be used for study of filamentation in the mid-IR. Another application of this setup is seeding high-pressure CO_2-laser amplifier [17]. It should be noted that presented setup of the mid-IR laser system is relatively simple and has a great potential for energy scalability. Energy of the front-end Ti:sapphire laser can be increased up to hundreds of Joules [12], however that pump laser will require a wide-aperture BGGSe crystal sample. Also, the DFG pulse energy can be increased by an improvement of signal pulse – uniform spectrum shape and increased energy.

Funding. Russian Science Foundation, grant number # 22-79-10068.

Conflict of interest. The authors of this work declare that they have no conflicts of interest.

1. K. Pogorelsky, I. Ben-Zvi, W. D. Kimura, N. A. Kurnit, and F. Kannari, Infrared Phys. Technol. **36**, 341 (1995).
2. C. Hernández-García, T. Popmintchev, M. M. Murnane, H. C. Kapteyn, L. Plaja, A. Becker, and A. Jaron-Becker, Opt. Express **25**, 11855 (2017).
3. A. A. Lanin, A. A. Voronin, A. B. Fedotov, and A. M. Zheltikov, Nature **4**, 6670 (2014).
4. N. A. Smirnov, Y. S. Gulina, N. I. Busleev, P. P. Pakholchuk, A. V. Gorevoy, V. G. Vins, and S. I. Kudryashov, JETP Lett. **119**, 411 (2024).
5. V. O. Kompanets, S. I. Kudryashov, E. R. Totordava, S. N. Shelygina, V. V. Sokolova, I. N. Saraeva, M. S. Kovalev, A. A. Ionin, and S. V. Chekalin, JETP Lett. **113**, 365 (2021).

6. I. O. Kinyaevskiy, A. A. Koribut, L. V. Seleznev, Yu. M. Klimachev, E. E. Dunaeva, and A. A. Ionin, Opt. Laser Technol. **169**, 110035 (2024).
7. R. T. Murray, T. H. Runcorn, E. J. R. Kelleher, and J. R. Taylor, Opt. Lett. **41**, 2446 (2016).
8. Y. Cui, H. Huang, Y. Bai, W. Du, M. Chen, B. Zhou, I. Jovanovic, and A. Galvanauskas, Opt. Lett. **48**, 1890 (2023).
9. U. Elu, L. Maidment, L. Vamos, T. Steinle, F. Haberstroh, V. Petrov, V. Badikov, D. Badikov, and J. Biegert, Opt. Lett. **45**, 3813 (2020).
10. W. Chen, L. Wang, I. B. Divliansky, V. Pasiskevicius, O. Mhibik, K. M. Moelster, A. Zukauskas, L. B. Glebov, and V. Petrov, Opt. Express **32**, 1728 (2024).
11. A. A. Ionin, I. O. Kinyaevskiy, Yu. M. Klimachev, A. A. Kotkov, A. Yu. Kozlov, A. M. Sagitova, D. V. Sinitsyn, V. V. Badikov, and D. V. Badikov, Opt. Laser Technol. **115**, 205 (2019).
12. W. Li, Z. Gan, L. Yu et al. (Collaboration), Opt. Lett. **43**, 5681 (2018).
13. V. V. Badikov, D. V. Badikov, V. B. Laptev, K. V. Mitin, G. S. Shevyrdyaeva, N. I. Shchebetova, and V. Petrov, Opt. Mater. Express **6**, 2933 (2016).
14. N. Kostyukova, E. Erushin, A. Boyko, G. Shevyrdyaeva, and D. Badikov, Photonics **11**, 281 (2024).
15. V. G. Dmitriev, G. G. Gurzadyan, and D. N. Nikogosyan, *Handbook of nonlinear optical crystals*, Springer (2013).
16. G. N. Patwardhan, J. S. Ginsberg, C. Y. Chen, M. M. Jadidi, and A. L. Gaeta, Opt. Lett. **46**, 1824 (2021).
17. M. N. Polyanskiy, I. V. Pogorelsky, M. Babzien, and M. A. Palmer, OSA Contin **3**, 459 (2020).